JOURNAL OF GUIDANCE, CONTROL, AND DYNAMICS
Vol. 21, No. 6, November–December 1998

Finite Time Stability Approach to Proportional Navigation Systems Analysis

Pini Gurfil,* Mario Jodorkovsky,† and Moshe Guelman‡
Technion—Israel Institute of Technology, 32000 Haifa, Israel

The finite time stability of proportional navigation guidance systems is considered. Assuming planar geometry and linear missile dynamics, a proportional navigation missile–target guidance model is first formulated. The model exhibits a feedback configuration consisting of a linear time-invariant element and a time-varying gain. The definition of finite time global absolute stability is then presented. It is shown that by employing the circle criterion, the finite time stability of the guidance dynamics can be analyzed. An analytic bound for the time of flight up to which stability can be assured is established. The bound depends on the system parameters and the time of flight. Less conservative results, as compared to previous works, are obtained. This approach enables not only analysis of the system behavior for given missile dynamics, but more importantly, enables generation of a tool for system design. Illustrative examples are presented showing the effect of the system parameters on the bound. In addition, some design implications, such as the relation to miss distance, are outlined.

Nomenclature

A = system matrix
a = lateral acceleration
B = system matrix
N = proportional navigation constant
N' = effective proportional navigation constant
R = missile–target line of sight
t_f = flight time (finite time)
V = velocity
V_C = closing velocity
γ = path angle
ζ = damping ratio
λ = line-of-sight angle
σ = system output
τ = time to go
τ_1 = missile time constant
ω = frequency
ω_n = natural frequency

Subscripts

c = commanded value
f = final value
M = missile
m = measured value
T = target
0 = initial value

Superscript

$\cdot$ = time differentiation

I. Introduction

PROPORTIONAL navigation (PN) is a commonly used method for missile guidance. A vast amount of literature exists on the subject (see, e.g., Ref. 1, and the references therein). Solutions of PN[2,3] indicate that for the case of ideal dynamics, i.e., no delays exist between the line-of-sight (LOS) rate and the applied acceleration, the LOS rate is a decreasing function of time converging to zero at the pursuit end. When actual dynamics are considered, it is known that PN guidance (PNG) tends to diverge at the vicinity of the interception,[4–7] i.e., the LOS rate diverges and, correspondingly, the required missile maneuver acceleration. This divergence may severely affect the miss distance. As such, it should constitute a major issue in missile design.

Many works have been conducted on the subject of miss distance analysis.[3] Missile guidance is a nonlinear control problem defined over a finite time interval. To apply known techniques of analysis the system equations are linearized. This linearization is valid close to the interception, when the missile reaches the so-called collision course. Effectively, close to pursuit end it was shown that the closing velocity approaches a constant value and the range can be approximated by a linear function of time.[2,3] Under this approximation, the system equations become linear and time varying. Using the linear time-varying equations, known techniques such as the adjoint method[3,8] were applied to perform miss distance analysis. The adjoint technique is based on the system impulse response and can be used to analyze miss distance by numerical integration in reverse time. In general, however, low-order simplified dynamics have been utilized, both for maneuvering and nonmaneuvering targets. Less attention has been paid to the interception phase stability problem taking into account more realistic models.

In a recent work,[5] the Kalman–Yakubovitch–Popov lemma was employed to investigate the finite time (absolute) stability of PNG systems. The underlying assumption in the work is that there is a strong connection between PNG system stability and miss distance. Although this assumption has not been analytically proven, its validity has been legitimized by empirical experience. In Ref. 5, an analytical expression relating the time up to which stability can be assured and the missile's parameters were developed. The analytical expression provides guidelines on how to attain larger times of stability by suitable system design. This approach enables not only the analysis of the system behavior for given missile dynamics, but more importantly, enables generation of a tool for system design.

This paper expands the results of Ref. 5. A linearized time-varying model of the guidance system is first obtained. An illustrative example shows its resemblance to the nonlinear model. Then, using the well-known circle criterion,[9–12] the finite time stability properties of PNG are investigated. Using this criterion, time-varying sectors of arbitrary size may be defined. This allows the formulation of sufficient conditions for stability for arbitrary flight times, thus improving the results in Ref. 5, where only the case of large flight times was considered. As the case of arbitrary flight times renders less conservative results, better bounds for the time of stability

Received Sept. 30, 1996; revision received May 19, 1997; accepted for publication May 29, 1998.

*Graduate Student, Department of Aerospace Engineering.
†Adjunct Teaching Associate, Department of Electrical Engineering, and Senior Research Scientist, RAFAEL, Israel Ministry of Defense, Department 39, P.O. Box 2250, 31021 Haifa, Israel.
‡Professor, Department of Aerospace Engineering.

are obtained. Moreover, the stability of the frozen time system is also imposed by the circle criterion. As this condition usually turns out to be much less conservative than others, it can be used as an indication of the limiting capabilities to attain long times of stability by autopilot design. We further show that the finite time absolute stability analysis can be employed to the design of autopilots that minimize the miss distance.

The paper is organized as follows: Section II presents the mathematical modeling used to analyze PNG systems. Section III outlines the circle criterion and introduces the concepts of absolute stability and finite time absolute stability. Section IV deals with finite time global absolute stability of PNG systems. In Sec. V some illustrative examples are considered, and in Sec. VI concluding remarks are given.

II. Mathematical Modeling

The general formulation of a three-dimensional PN interception problem is rather complicated. However, assuming that the lateral and longitudinal maneuver planes are decoupled by means of roll control, one can deal with the equivalent two-dimensional problem in quite a realistic manner. We shall further assume that the geometry is two-dimensional. In addition to this basic assumption, we shall also assume that the gravitational component of the total missile lateral acceleration is negligible.

The preceding assumptions enable us to formulate a general planer intercept missile–target geometry as shown in Fig. 1. The figure describes a missile employing PN to intercept a maneuvering target. It could be either true proportional navigation (TPN), where the maneuver acceleration is perpendicular to the instantaneous LOS, or pure proportional navigation (PPN), where the maneuver acceleration is perpendicular to the instantaneous velocity vector. In both cases the mathematical treatment is similar. It only depends on how the effective PN constant is defined, as we shall see subsequently.

The kinematic equations of motion modeling the geometry given in Fig. 1 are

$$\begin{aligned} \dot{R} &= V_T \cos(\lambda - \gamma_T) - V_M \cos\delta \\ R\dot{\lambda} &= V_T \sin(\lambda - \gamma_T) - V_M \sin\delta, \qquad \delta = \gamma_M - \lambda \end{aligned} \tag{1}$$

Under the assumptions that the deviations from collision course are small and the closing velocity V_C is constant, we can write

$$\dot{R} = V_T \cos(\lambda - \gamma_T) - V_M \cos\delta \triangleq -V_C \approx \text{const} \tag{2}$$

$$R = V_C \cdot \tau \tag{3}$$

where τ is the time to go, given by

$$\tau = t_f - t, \qquad t_f = R_0/V_C \tag{4}$$

The commanded missile acceleration generated by the PN control law is

$$a_C = N' V_C \dot{\lambda}_m \tag{5}$$

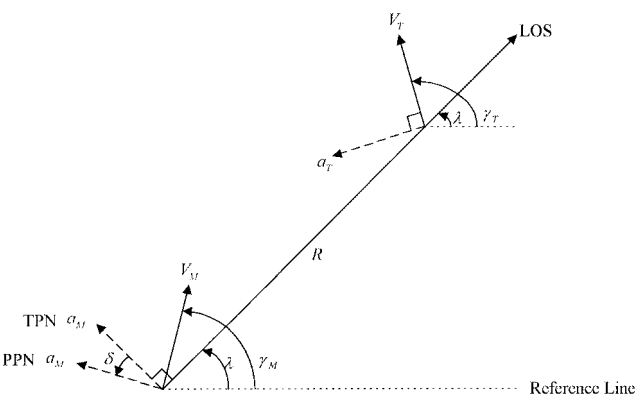

Fig. 1 Planar intercept geometry.

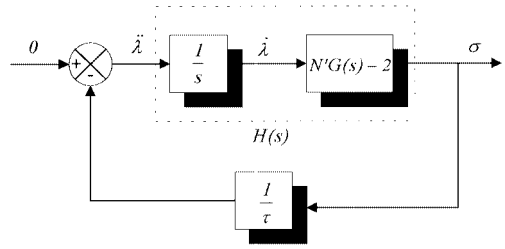

Fig. 2 Representation of a PNG loop.

where $\dot{\lambda}_m$ is the measured LOS rate and N' is the effective PN constant given by

$$N' = \begin{cases} N V_M \cos\delta / V_C & \text{for} \quad \text{PPN} \\ N V_M / V_C & \text{for} \quad \text{TPN} \end{cases} \tag{6}$$

The seeker dynamics is modeled by the transfer function $G_1(s)$

$$G_1(s) = \frac{\dot{\lambda}_m(s)}{\dot{\lambda}(s)} \tag{7}$$

The missile's flight control dynamics is described by the transfer function $G_2(s)$

$$G_2(s) = \frac{a_M(s)}{a_c(s)} \tag{8}$$

From Eqs. (5), (7), and (8) the overall closed-loop dynamics between the LOS rate and the actual missile acceleration is described by the transfer function

$$\tilde{G}(s) = N' V_C G_1(s) G_2(s) = N' V_C G(s) \tag{9}$$

It is assumed that $G(s) = G_1(s) \cdot G_2(s)$ is asymptotically stable.

The general equation describing the missle acceleration normal to the LOS (see Fig. 1) includes the angular acceleration and the Coriolis effect. From basic kinematics, this equation is

$$R\ddot{\lambda} + 2\dot{R}\dot{\lambda} = -a_M + a_T \tag{10}$$

Now, substituting Eqs. (3), (5), and (9) into Eq. (10) gives

$$\tau\ddot{\lambda}(t) - 2\dot{\lambda}(t) = -N' G(s)\dot{\lambda}(t) + a_T/V_C \tag{11}$$

where the usual notation has been adopted.

From Eq. (11) we can express the LOS acceleration as

$$\ddot{\lambda}(t) = (1/\tau)\{[2 - N' G(s)] \cdot \dot{\lambda}(t) + a_T/V_C\} \tag{12}$$

The stability of the linearized two-dimensional PN system can be analyzed by manipulating Eq. (12) to obtain a closed-loop system representation consisting of a linear time-invariant (LTI) element in the forward path and a time-varying gain in the feedback. The closed-loop system is shown in Fig. 2. In Fig. 2, it is implicitly assumed that $a_T = 0$. This assumption shall be referred to later in the study. The LTI portion is $H(s)$. Notice that the feedback is the kinematic gain $1/\tau$. The output of the system is σ, where

$$\sigma(t) = [N' G(s) - 2] \cdot \dot{\lambda}(t) \tag{13}$$

It is already possible to state that, because the loop gain $1/\tau$ increases monotonically with time, at a certain time before interception (frozen time) instability will occur. In the next section, this issue will be discussed.

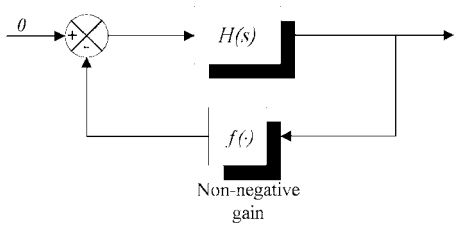

Fig. 3 System under investigation.

III. Absolute Stability, Finite Time Absolute Stability, and the Circle Criterion

Consider the feedback configuration of Fig. 3. Figure 3 shows a zero input control loop containing an LTI transfer function in the forward path and a single, nonnegative nonlinear time-varying gain in the feedback. By a suitable selection of the state vector[13] the governing differential equations can be expressed in the form

$$\frac{\mathrm{d}}{\mathrm{d}t}x(t) = Ax(t) + f(x,t)Bx(t) \tag{14}$$

The $n \times n$ matrix A is of lower companion form, and the $n \times n$ matrix B has rank one:

$$A = \begin{bmatrix} 0 & 1 & \cdots & 0 \\ \vdots & 0 & & \vdots \\ 0 & 0 & \cdots & 1 \\ -a_n & -a_{n-1} & \cdots & -a_1 \end{bmatrix} \qquad B = \begin{bmatrix} 0 & 0 & \cdots & 0 \\ \vdots & \vdots & & \vdots \\ 0 & 0 & \cdots & 0 \\ -b_{n-1} & -b_{n-2} & \cdots & -b_0 \end{bmatrix} \tag{15}$$

The real constants a_i, $i = 1, 2, \ldots, n$ and b_j, $j = 0, 1, \ldots, n-1$, are the coefficients of the polynomials

$$q(s) = b_0 s^{n-1} + b_1 s^{n-2} + \cdots + b_{n-1}$$
$$p(s) = s^n + a_1 s^{n-1} + \cdots + a_n \tag{16}$$

The stability information obtained from the circle criterion applies to the class of functions $f(\cdot)$ constrained in the interval $[\alpha, \beta]$, i.e.,

$$0 \le \alpha \le f(x,t) \le \beta < \infty, \qquad \forall x \in \Re^n, \quad \forall t \ge t_0 \tag{17}$$

The class of differential systems given by Eqs. (14) and (17) shall be denoted $D_{\alpha,\beta}$.

Now consider the following definition.

Definition 1: System (14) is globally absolutely stable (asymptotically stable) if there exists $P > 0$ such that $\|x(t)\|_P \triangleq x^T(t)Px(t)$ is a nonincreasing (decreasing) function of time $\forall x(t_0)$, $\forall t \ge t_0$.

Regarding Fig. 3, it is assumed that 1) $H(s) = q(s)/p(s)$, $p(s)$ and $q(s)$ are coprime polynomials, $p(s)$ is monic and $H(s)$ is stricly proper, i.e., $\deg[p(s)] > \deg[q(s)]$ and 2) the gain $f(\cdot)$ is an operator $f(x,t)$: $\Re^n \times J \to \Re_+$, $J \triangleq [t_0, \infty)$, which is a function of the time and perhaps some state variables. It is also smooth enough to guarantee the existence and uniqueness of a solution to the governing differential equations for any initial conditions.

Under these assumptions the following theorem gives sufficiency conditions for global absolute stability (GAS) and global absolute asymptotic stability (GAAS).

Theorem 1 (circle criterion[9,10]):

1) Every differential system in class $D_{\alpha,\beta}$ is GAS if a) $p(s)+kq(s)$ has no zeros in the right half-plane $\mathrm{Re}[s] > 0$ for any $k \in [\alpha, \beta]$, and its imaginary axis $\mathrm{Re}[s] = 0$ zeros are simple; and b)

$$\mathrm{Re}\{[p(-j\omega) + \alpha q(-j\omega)] \cdot [p(j\omega) + \beta q(j\omega)]\} \ge 0, \qquad \forall \omega \in \Re$$

2) Every differential system in class $D_{\alpha,\beta}$ is GAAS if a) $p(s)+\alpha q(s)$ has all of its zeros in the left half-plane $\mathrm{Re}[s] < 0$; and b)

$$\mathrm{Re}\{[p(-j\omega) + \alpha q(-j\omega)] \cdot [p(j\omega) + \beta q(j\omega)]\} \ge 0, \qquad \forall \omega \in \Re$$

The circle criterion is well known. Theorem 1 may be used in the context of input–output (L_2) stability[11] or internal Lyapunov stability.[9,10,14] It can be proved in several ways, e.g., by using quadratic Lyapunov functions.[9]

Remark: In the preceding formulation of the circle criterion, a zero input system was assumed. However, Theorem 1 holds also in the bounded-input bounded-output sense.[11] This is true because the circle criterion provides sufficiency conditions not only for asymptotic stability but, moreover, for exponential stability.[11,12] Thus, although we implicitly assumed that $a_T = 0$ to obtain the canonical form shown in Fig. 2, this was done mainly to obtain a more useful representation. No loss of generality occurs when assuming $a_T = 0$.

Now, let J_t be the time interval $[t_0, t]$. Consider the function $f(x,t) = 1/(t_f - t)$, $t \in J_{t_f} \triangleq [t_0, t_f]$. For this case, where the time is defined over a finite interval, we may define the following.

Definition 2 (Ref. 5): System (12) is finite time globally absolutely stable (asymptotically stable) in the interval $J_{t^*} = [t_0, t^*] \subseteq J_{t_f}$ if there exists $P > 0$ such that $\|x(t)\|_P$ is a nonincreasing (decreasing) function of time $\forall x(t_0)$, $\forall t \in J_{t^*}$.

In the next section, the finite time global absolute stability (FTGAS) of PNG systems is investigated.

IV. FTGAS of PNG Systems

The reader may have noticed by now that the formulation of the circle criterion discussed in Sec. III and the mathematical modeling of the PNG system presented are in close relation. To investigate the FTGAS properties of the PNG system we first notice that the LTI portion of the system is given by

$$H(s) = q(s)/p(s) = (1/s)[N'G(s) - 2] \tag{18}$$

and that the nonlinear element $f(x,t)$ is the linear time-varying kinematic gain $1/\tau$ (recall that τ is the time to go defined as $\tau = t_f - t$).

We now consider the interval

$$0 \le \alpha = 1/t_f \le 1/\tau \le 1/\tau^* = \beta \tag{19}$$

where $\tau^* = 1/\beta$ is the shortest time to go for which the guidance loop of Fig. 2 is stable in the sense of Definition 2, i.e., τ^* provides a lower bound for the time to go for which guidance divergence might occur. The calculation of this bound provides important information for the analysis of PNG systems, as will be elaborated on later. We shall now apply the conditions of Theorem 1 to the PNG system described in Fig. 2 and Eqs. (18) and (19). First, it is necessary to show that $q(s)$ and $p(s)$ are coprime. This will be done by means of the following lemma:

Lemma 1: Assume $G(s) = n(s)/d(s)$ with $n(s)$ and $d(s)$ coprime and $G(0) = 1$. Define as in Eq. (18) $H(s) = q(s)/p(s) = (1/s)[N'G(s) - 2]$. Then, if $N' \ne 2$, $p(s)$ and $q(s)$ are coprime.

Proof: See Appendix A.

We shall now examine the immediate consequences that result from conditions 1a and 2a of Theorem 1. In fact, the conditions state that the frozen time ($t = \text{const}$) closed-loop system should be stable (asymptotically stable) at all times in the interval J_{t^*}; i.e., one should examine whether or not the system matrix $A + kB$ is Hurwitz (strictly Hurwitz) at each frozen time point $t = 1/k$, $k \in [\alpha, \beta] = [1/t_f, 1/(t_f - t^*)]$. Now, consider the characteristic equation of the closed-loop system shown in Fig. 3, where the time-varying gain is frozen at a value $k \in [\alpha, \beta]$

$$1 + kH(s) = 1 + (k/s)[N'G(s) - 2] = 0 \tag{20}$$

or

$$s + k[N'G(s) - 2] = 0 \tag{21}$$

Because $G(0) = 1$, the characteristic equation (21) can be written as

$$r(s) + k[N' - 2] = 0 \tag{22}$$

Where the polynomial $r(s)$ has no free terms, i.e., $r(0) = 0$. From Eq. (22) it is seen that for conditions 1a or 2a of Theorem 1 to hold, it is necessary that

$$N' > 2 \tag{23}$$

Condition (23) is well known for PN, but the treatment used here to establish it is novel.

For the examination of conditions 1b and 2b of Theorem 1, we first notice for $\omega = 0$ that $p(0) = 0$. Also, because $\alpha, \beta \geq 0$, these conditions reduce to the condition $\alpha\beta|\alpha(0)|^2 \geq 0$, which is trivially satisfied. Now, suppose $\omega \neq 0$. Because $G(s)$ is asymptotically stable, $p(j\omega) \neq 0 \ \ \forall\omega \neq 0$ and conditions 1b and 2b can be written as

$$\mathrm{Re}\left\{|p(j\omega)|^2\left[1 + \alpha\frac{q(-j\omega)}{p(-j\omega)} + \beta\frac{q(j\omega)}{p(j\omega)} + \alpha\beta\frac{q(-j\omega)}{p(-j\omega)}\cdot\frac{q(j\omega)}{p(j\omega)}\right]\right\} \geq 0, \qquad \forall\omega \neq 0 \tag{24}$$

where $\alpha = 1/t_f$.

Equivalently, we write Eq. (24) as

$$\mathrm{Re}[1 + \alpha H(-j\omega) + \beta H(j\omega) + \alpha\beta|H(j\omega)|^2] \geq 0, \qquad \forall\omega \neq 0 \tag{25}$$

Now, suppose that there exists an $\omega^* \neq 0$ such that $\mathrm{Re}[1 + \alpha H(j\omega^*)] = 0$. In this case, and because $\beta \neq 0$, Eq. (25) reduces to

$$\mathrm{Re}[H(j\omega^*) + \alpha|H(j\omega^*)|^2] \geq 0 \tag{26}$$

or

$$\alpha^2|H(j\omega^*)|^2 \geq 1 \tag{27}$$

Substituting the equality $\mathrm{Re}[H(j\omega)] = -1/\alpha$ into Eq. (27) yields the condition $-(1/\alpha) + \alpha\mathrm{Re}^2[H(j\omega)] + \alpha\mathrm{Im}^2[H(j\omega)] = \alpha\mathrm{Im}^2[H(j\omega)] \geq 0$, which is always satisfied. Consequently, we shall define

$$\Omega_\alpha^* = \{\omega^* : 1 + \alpha\,\mathrm{Re}\,[H(j\omega^*)] = 0 \quad \text{or} \quad \omega^* = 0\} \tag{28}$$

and consider only frequencies $\omega \in \Omega_\alpha = \Re - \Omega_\alpha^*$.

Lemma 2: If the PNG system is frozen time closed-loop stable (asymptotically stable) in some interval J_t, then $1 + \alpha\mathrm{Re}[H(j\omega)] \geq 0 \ \ \forall\omega \in \Omega_\alpha$.

Proof: If conditions 1a or 2a hold, the polynomial $p(s) + \alpha q(s)$ is Hurwitz. Because $H(j\omega) = q(j\omega)/p(j\omega)$ then by the Nyquist stability theorem $\mathrm{Re}[H(j\omega)] \geq -1/\alpha \ \ \forall\omega \in \Omega_\alpha$. □

Next, using Lemma 2, we manipulate Eq. (25) to obtain

$$\frac{\mathrm{Re}[H(j\omega)] + \alpha|H(j\omega)|^2}{1 + \alpha\mathrm{Re}[H(j\omega)]} \geq -\frac{1}{\beta}, \qquad \forall\omega \in \Omega_\alpha \tag{29}$$

which can be written in the form

$$\frac{N'\mathrm{Re}[G(j\omega)/j\omega] + \alpha|H(j\omega)|^2}{1 + \alpha N'\mathrm{Re}[G(j\omega)/j\omega]} \geq -\frac{1}{\beta}, \qquad \forall\omega \in \Omega_\alpha \tag{30}$$

By Eq. (30) and Theorem 1, the system is FTGAS (FTGAAS) in the interval J_{t^*} if it is frozen time closed-loop stable (asymptotically stable), and in this interval

$$\tau \geq -\frac{N'\mathrm{Re}[G(j\omega)/j\omega] + \alpha|H(j\omega)|^2}{1 + \alpha N' Re[G(j\omega)/j\omega]} \triangleq -f_\alpha(\omega), \qquad \forall\omega \in \Omega_\alpha \tag{31}$$

The lower bound on the time to go is, thus,

$$\tau_\alpha = \min_{\omega \in \Omega_\alpha} f_\alpha(\omega) \tag{32}$$

The expression presented in Eq. (32) expands the results obtained in Ref. 5. From an engineering point of view, it provides an estimate to the divergence time of the system states for given flight time and system parameters.

Lemma 2 will be also used for the proof of the following proposition.

Proposition: Here $f_{\alpha_2}(\omega) \geq f_{\alpha_1}(\omega) \ \ \forall\alpha_2 \geq \alpha_1, \ \forall\omega \in \Omega_{\alpha_{12}} = \Omega_{\alpha_1} \cap \Omega_{\alpha_2}$.

Proof: Let $\phi(j\omega) \triangleq N'G(j\omega)/j\omega$. We need to show that

$$\frac{\mathrm{Re}[\phi(j\omega)] + \alpha_1|\phi(j\omega) + 2j/\omega|^2}{1 + \alpha_1\mathrm{Re}[\phi(j\omega)]} \leq \frac{\mathrm{Re}[\phi(j\omega)] + \alpha_2|\phi(j\omega) + 2j/\omega|^2}{1 + \alpha_2\mathrm{Re}[\phi(j\omega)]} \qquad \forall\alpha_1 \leq \alpha_2, \quad \omega \in \Omega_{\alpha_{12}}$$

By Lemma 2, $1 + \alpha_i\mathrm{Re}[H(j\omega)] = 1 + \alpha_i\mathrm{Re}[f(j\omega)] > 0 \ \ \forall\omega \in \Omega_{\alpha_i}$; therefore, the preceding expression can be written as

$$\alpha_1\{|\phi(j\omega) + 2j/\omega|^2 - \mathrm{Re}^2[\phi(j\omega)]\} \leq \alpha_2\{|\phi(j\omega) + 2j/\omega|^2 - \mathrm{Re}^2[\phi(j\omega)]\} \qquad \forall\alpha_1 \leq \alpha_2, \quad \forall\omega \in \Omega_{\alpha_{12}}$$

which is always satisfied. □

From the preceding proposition it turns out that for longer flight times, the time-to-go lower bound becomes more conservative, as will be shown in the next corollary:

Corollary 1: Here $\tau_{\alpha_2} \leq \tau_{\alpha_1}$ for all $\alpha_2 \geq \alpha_1$.

Proof: Because $f_{\alpha_2}(\omega) \geq f_{\alpha_1}(\omega) \ \ \forall\alpha_2 \geq \alpha_1, \omega \in \Omega_{\alpha_{12}}$, then

$$\min_{\omega \in \Omega_{\alpha_{12}}} f_{\alpha_1}(\omega) \leq \min_{\omega \in \Omega_{\alpha_{12}}} f_{\alpha_2}(\omega), \qquad \forall\alpha_2 \geq \alpha_1$$

And, therefore,

$$\tau_{\alpha_2} = -\min_{\omega \in \Omega_{\alpha_{12}}} f_{\alpha_2}(\omega) \leq -\min_{\omega \in \Omega_{\alpha_{12}}} f_{\alpha_1}(\omega) = \tau_{\alpha_1}, \qquad \forall\alpha_2 \geq \alpha_1 \quad \square$$

From Corollary 1 we conclude that the longer the flight time $t_f = 1/\alpha$ is, the more conservative becomes the bound τ_α. This result should not be surprising, because as flight times increase, the nonlinearity sectors in the formulation of the circle criterion become larger. Notice also that for small flight times the loop gain becomes large, and conditions 1a and 2a of Theorem 1 may be violated.

When t_f is large, α is small. We will consider here the limiting case $\alpha \to 0$, which simplifies the mathematical treatment substantially.[5] Also, because $0 \leq 1/\tau \ \ \forall t_f$, one might choose $\alpha \to 0$ when t_f is unknown. Letting $\alpha \to 0$, Theorem 1 conditions 1b and 2b can be approximated by the inequality

$$\mathrm{Re}[p(-j\omega)\cdot p(j\omega) + \beta p(-j\omega)\cdot q(j\omega)] \geq 0, \qquad \forall\omega \neq 0 \tag{33}$$

Expression (33) can be written as

$$\mathrm{Re}\left\{|p(j\omega)|^2\left[1 + \beta\frac{q(j\omega)}{p(j\omega)}\right]\right\} = |p(j\omega)|^2\mathrm{Re}\left[1 + \beta\frac{q(j\omega)}{p(j\omega)}\right] \geq 0, \qquad \forall\omega \neq 0 \tag{34}$$

which reduces to

$$\mathrm{Re}[H(j\omega)] \geq -(1/\beta), \qquad \forall\omega \neq 0 \tag{35}$$

Because by Eq. (18) $H(j\omega) = [N'G(j\omega)/j\omega] - (2/j\omega)$, and by Eq. (19) $1/\beta \leq \tau$, Eq. (35) can be written as

$$\tau \geq -N' \cdot \mathrm{Re}\left[\frac{G(j\omega)}{j\omega}\right] \triangleq -f_0(\omega), \qquad \forall\omega \neq 0 \tag{36}$$

The expression in Eq. (36) is identical to that obtained in Ref. 5. It implies that for any flight time the PNG system is FTGAS (FTGAAS), in the sense of Theorem 1, as long as the system is closed-loop frozen time stable (asymptotically stable) and the time to go is not shorter than

$$\tau_0 = -\min_{\omega \neq 0} f_0(\omega) \tag{37}$$

Note that $f_0(\omega) = f_{\alpha \to 0}(\omega)$.

It is emphasized that the FTGAS (FTGAAS) analysis holds also when any input, such as target maneuver, is employed in the PNG system. This is in accordance with the stated Remark.

V. Illustrative Examples

Example 1: Consider a missile whose dynamics are modeled by the product of first-order systems, i.e.,

$$G(s) = \prod_{i=1}^{n} \frac{1}{\tau_i s + 1}$$

It can be shown (see Appendix B) that for such systems the bound τ_0 is given by

$$\tau_0 = N' \sum_{i=1}^{n} \tau_i \tag{38}$$

For illustration, consider a PNG system with a single time constant, i.e., $G(s) = 1/(\tau_1 s + 1)$. The closed-loop characteristic equation is

$$\tau_1 \tau \dddot{\lambda} + (\tau - 2\tau_1)\ddot{\lambda} + (N' - 2)\dot{\lambda} = 0 \tag{39}$$

By Eq. (39), the frozen time stability is guaranteed for

$$\tau > 2 \cdot \tau_1, \qquad N' > 2 \tag{40}$$

Assuming large flight time, the bound Eq. (38) gives

$$\tau > N' \tau_1 \tag{41}$$

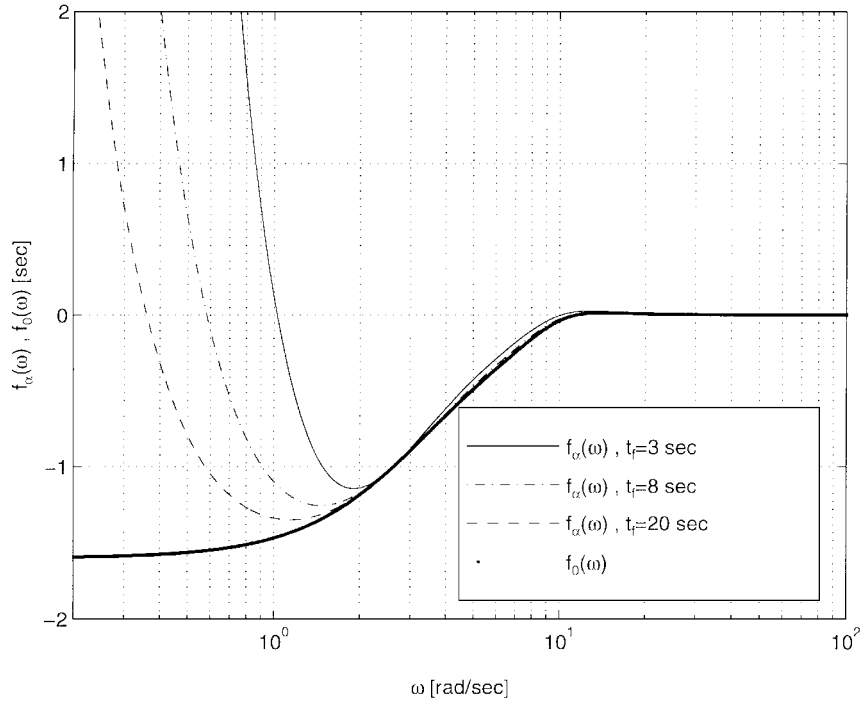

Fig. 4 Plots of $f_\alpha(\omega)$ and $f_0(\omega)$ for $N' = 4$, $\tau_1 = 0.3$ s, $\zeta = 0.5$, and $\omega_n = 10$ rad/s.

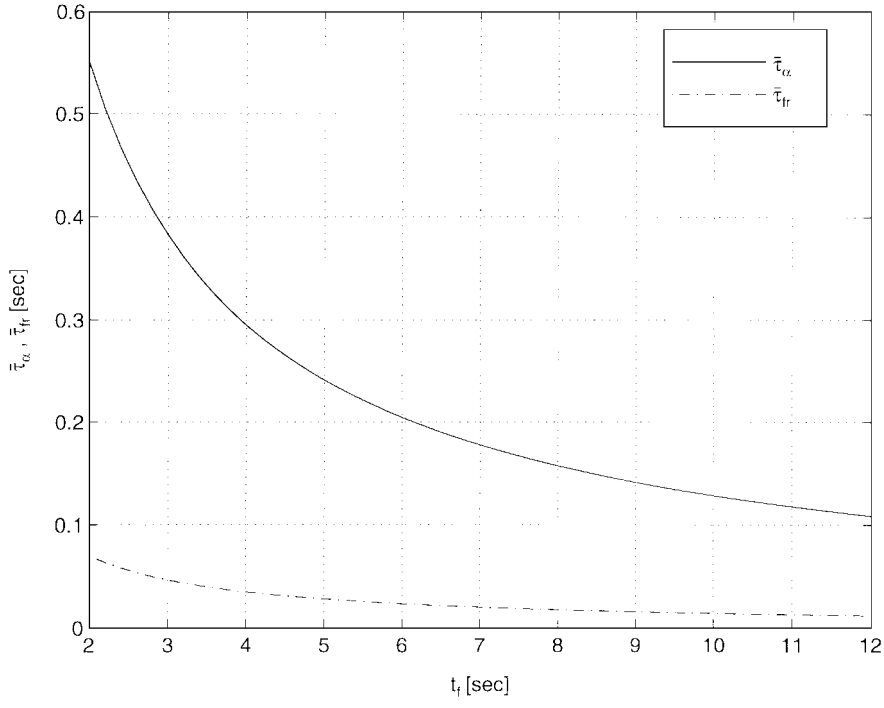

Fig. 5 Plots of $\bar{\tau}_\alpha$ and $\bar{\tau}_{fr}$ as functions of flight time for $N' = 4$, $\tau_1 = 0.3$ s, $\zeta = 0.5$, and $\omega_n = 10$ rad/s.

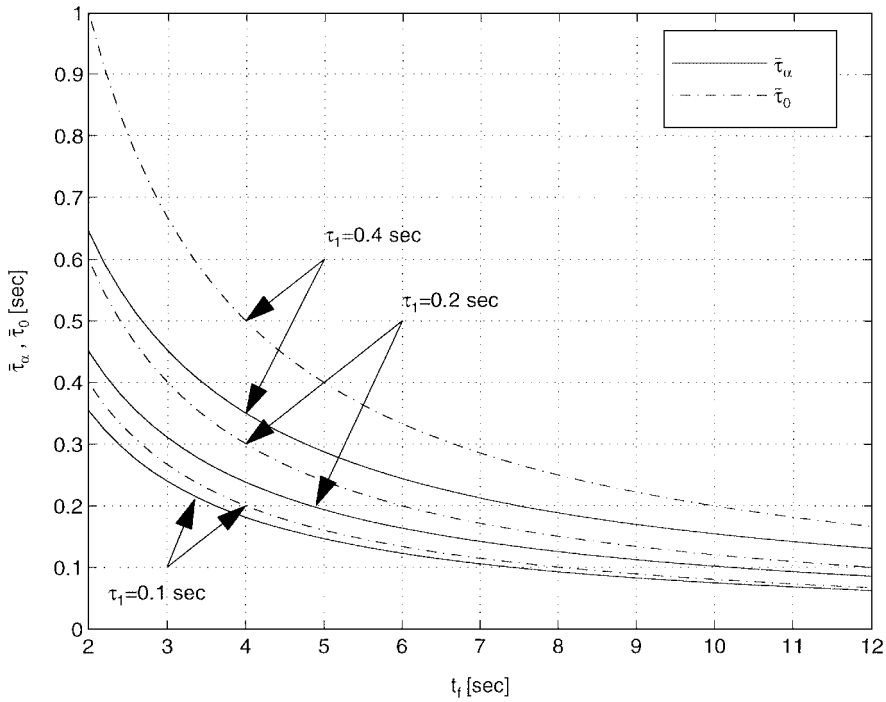

Fig. 6 Plots of $\bar{\tau}_\alpha$ and $\bar{\tau}_0$ as functions of flight time with τ_1 as the parameter and $N' = 4$, $\zeta = 0.5$, and $\omega_n = 10$ rad/s.

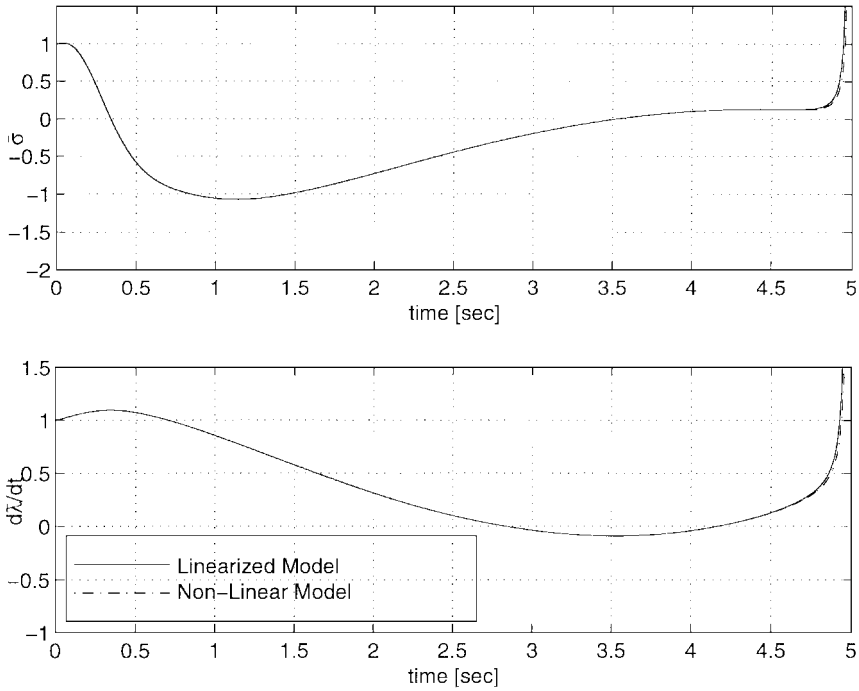

Fig. 7 Time histories of $\bar{\sigma} = \sigma/\sigma_0$ and $\dot{\bar{\lambda}} = \dot{\lambda}/\dot{\lambda}_0$ for $N' = 4$, $\tau_1 = 0.3$ s, $\zeta = 0.5$, $\omega_n = 10$ rad/s, and $t_f = 5$ s.

Thus, because it is required that $N' > 2$, the FTGAS of the system is determined by Eq. (41). Consequently, the frozen time stability condition (40) provides the least conservative requirement. Note also that to obtain the best system performance from stability considerations it is advisable to choose the smallest N' above 2.

Example 2: To further illustrate the results obtained, consider a missile whose tracking system is modeled by a single time constant τ_1 and whose flight control system is modeled by a second-order transfer function with damping ζ and natural frequency ω_n. The missile overall transfer function is, therefore, given by

$$G(s) = \frac{a_M(s)}{\dot{\lambda}(s)} = \frac{1}{(\tau_1 s + 1) \cdot \left(s^2/\omega_n^2 + 2\zeta s/\omega_n + 1\right)} \tag{42}$$

Assuming $N' = 4$, $\tau_1 = 0.3$ s, $\zeta = 0.5$, and $\omega_n = 10$ rad/s, Fig. 4 shows plots of $f_0(\omega)$ and of $f_\alpha(\omega)$ for $t_f = 3$, 8, and 20 s. It can be seen that for the system parameters just given, the bound τ_α (which is the negative of the minimum value of the plots) is sensitive to flight time. In the case examined, we have $\tau_\alpha = 1.14$ s for flight time of 3 s and $\tau_0 = 1.6$ s for a very large flight time, a difference of 40%.

Next, recall that in addition to the sufficient condition (32) for the system's FTGAS (FTGAAS) the closed loop is required to be frozen time stable (asymptotically stable).

The time to go where this is no longer true is τ_{fr}. The normalized quantity is τ_{fr}/t_f and is $\bar{\tau}_{fr}$. Many popular linear design techniques utilized to obtain desirable system end-game performance are based on frozen time, classical methods. Thus, it is interesting

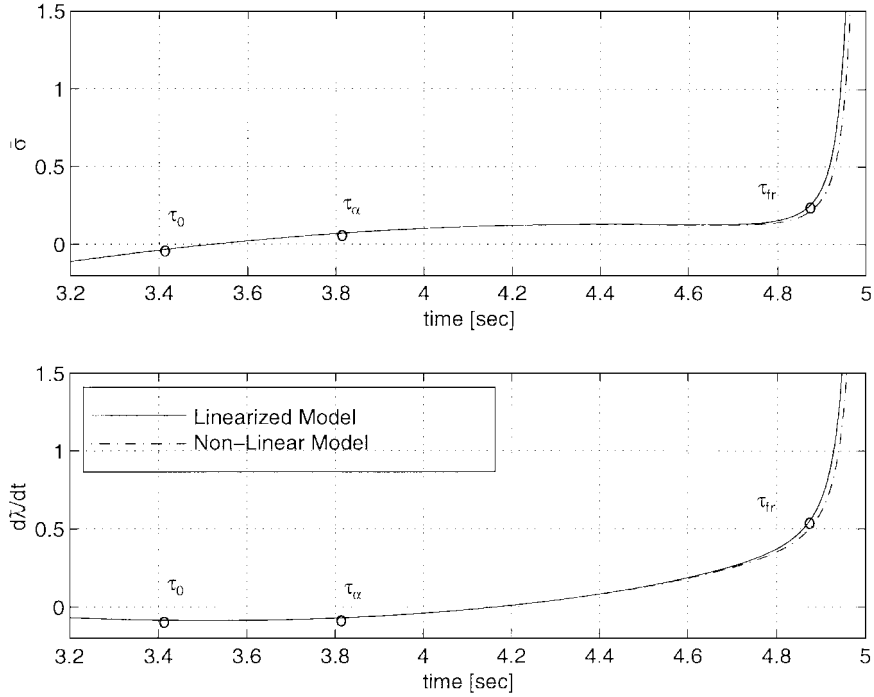

Fig. 8 Close-up of Fig. 7 to show the bounds τ_{fr}, τ_α, and τ_0.

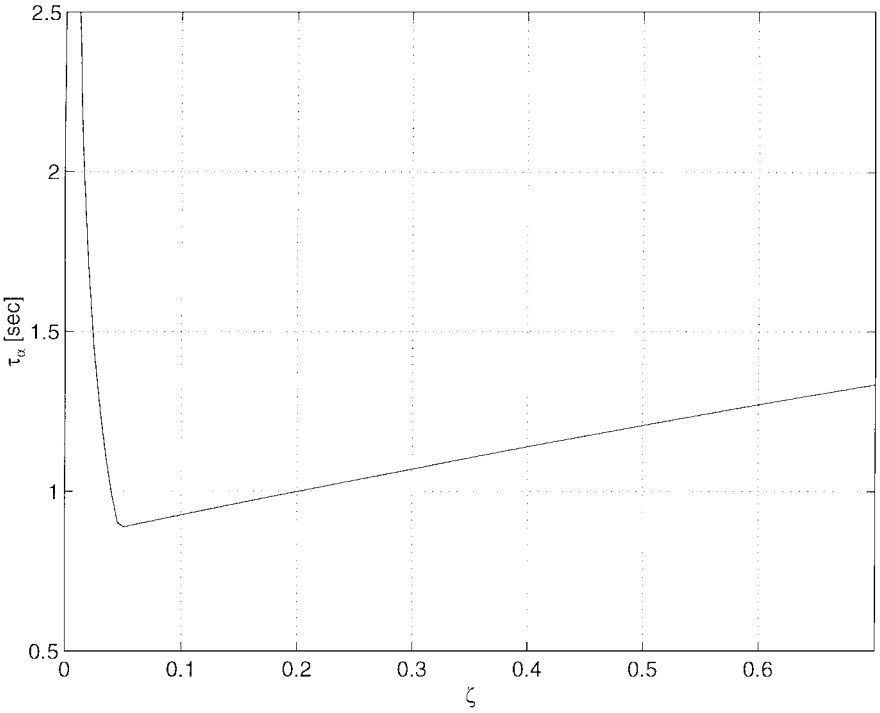

Fig. 9 Bound τ_α vs ζ for t_f = 5 s, N' = 4, τ_1 = 0.3 s, and ω_n = 10 rad/s.

to investigate the relationship between the two sufficient conditions of Theorem 1. In Fig. 5 we show $\bar{\tau}_\alpha = \tau_\alpha / t_f$ and $\bar{\tau}_{fr}$ as functions of flight time for the system parameters given earlier. Note that although the bound τ_α is an increasing function of the flight time, the normalized bound $\bar{\tau}_\alpha$ decreases with flight time, as physical intuition dictates. Figure 5 also shows that for the described system the bound generated by Eq. (32) is more conservative than the requirement on the system closed-loop frozen time stability (asymptotic stability); i.e., the system's frozen time stability (asymptotic stability) does not guarantee FTGAS (FTGAAS) in the sense of Theorem 1, because assertions 1b and 2b of Theorem 1 do not hold.

Let now $\bar{\tau}_0 = \tau_0 / t_f$ be the normalized quantity of the bound (37). In Fig. 6, we investigate the difference between the bounds $\bar{\tau}_\alpha$ and $\bar{\tau}_0$ as functions of the flight time with τ_1 as the parameter. The purpose of this is to establish the differences between the former bound obtained in Ref. 5 and the new bound derived in Eq. (32). The bound $\bar{\tau}_0$ is calculated as follows: First we calculate τ_0 according to Eq. (37); then we normalize it by the actual flight times. The figure raises two consequences: 1) For systems with large time constants operating over small time intervals, the result obtained assuming large flight time (the bound $\bar{\tau}_0$) is quite conservative. 2) It is apparent that $\bar{\tau}_\alpha \leq \bar{\tau}_0$, which agrees with Corollary 1.

To illustrate the tightness of the various bounds presented, the time histories of the normalized quantities $\bar{\sigma} = \sigma / \sigma_0$ and $\bar{\lambda} = \dot{\lambda} / \dot{\lambda}_0$ for flight time of 5 s and the parameters chosen earlier are shown in Fig. 7. In Fig. 7 we compare simulations of both the nonlinear and the linearized models as presented in Sec. I. It is apparent that both the linear and the nonlinear models are very close to each other. In particular, they exhibit a similar divergence behavior at the vicinity of the interception phase.

In Fig. 8 a close-up of Fig. 7 was made. The bounds τ_{fr}, τ_α, and τ_0 are marked. From Fig. 8 it is clear that the bound τ_{fr}, calculated according to frozen time closed-loop stability, is not reliable enough; in fact, it predicts a divergence time deep inside the divergence phase. Figure 8 also shows that the bound τ_α gives a reasonable estimate to the divergence time, whereas the bound τ_0 is more conservative. Note that because the lateral acceleration lags the LOS rate, the divergence of the LOS rate occurs earlier than the divergence of the lateral acceleration.

Example 3: We shall conclude this section with an example that outlines a possible design procedure employing finite time stability methods. Consider system (42) with $t_f = 3$ s, $N' = 4$, $\tau_1 = 0.3$ s, $\omega_n = 10$ rad/s, and $\dot{\lambda}_0 = 0.5$ deg/s. Assume also that the target performs a constant 5-g escape maneuver (recall that according to the Remark, the FTGAAS analysis holds also in the bounded-input bounded-output sense).

It is desired to choose ζ such that divergence is postponed as much as possible. This problem may be solved either analytically, by finding $\tau_{\alpha_{\min}} = \min_\zeta \tau_\alpha(\zeta)$, or graphically, by drawing τ_α vs ζ. We chose the latter method. Thus, in Fig. 9 we show τ_α vs ζ for the system parameters mentioned. It is seen that $\zeta \approx 0.05$ gives $\tau_\alpha \approx 0.89$, which is the minimum value. Consequently, it is expected that choosing $\zeta \approx 0,05$ will yield a superior stability performance. This conjecture was tested by simulation. In Fig. 10 we shown $\bar{\dot{\lambda}} = \dot{\lambda}/\dot{\lambda}_0$ vs time for $\zeta = 0.02, 0.05$, and 0.7. Note that $\zeta = 0.05$ corresponds to the system with the longest time of stability. It should be remarked that this value of ζ is smaller than the values usually assumed to be required when flight control system design is performed by other methods.

The value of ζ that was chosen in the preceding paragraph, based on FTGAAS analysis, also yields a smaller miss distance. We remind the reader that the miss distance is defined as

$$y_f \triangleq \lim_{t \to t_f} [V_C \cdot (t_f - t) \cdot \dot{\lambda}(t)] \tag{43}$$

Table 1 Miss distance for various damping coefficients

Miss distance y_f, m	Damping coefficient ζ
−0.17	0.02
−0.14	0.05
−1.7	0.7

For a 5-g target maneuver, we obtain the miss values given in Table 1. Note that $\zeta = 0.05$ gives the smaller miss distance. Thus, by choosing the damping coefficient that exhibits the best stability behavior, a smaller miss distance is obtained. Consequently, the FTGAAS analysis also may be utilized for miss distance minimization.

VI. Concluding Remarks

A linearized model of a PNG system including a missile dynamic of arbitrary order was presented. The theory of global absolute stability was utilized to define the FTGAS of a PNG system. The circle criterion was applied to establish a lower bound on the system's time to go before divergence. The bound is less conservative than the bound established in a previous work. Some illustrative examples were presented, showing the effect of a system's parameters and flight time on the calculated bound. The analytical expression for the bound provides guidelines for system design, such as choosing autopilot parameters for miss-distance minimization.

Appendix A: Proof of Lemma 1

To prove Lemma 1, we shall introduce the following lemma.

Lemma: Given two polynomials $a(z)$ and $b(z)$ with $\deg a(z) = n$ and $\deg b(z) = m, m < n$, and four constants c_1, c_2, c_3, and c_4 with $c_1c_4 - c_2c_3 \neq 0$, then the polynomials $c_1a(z) + c_2b(z)$ and $c_3a(z) + c_4b(z)$ are coprime.

Proof: Because $a(z)$ and $b(z)$ are coprime, there exist unique polynomials $\hat{x}(z)$ and $\hat{y}(z)$ with $\deg \hat{x}(z) < m$ and $\deg \hat{y}(z) < n$ such that the Bezout identity

$$\hat{x}(z)a(z) + \hat{y}(z)b(z) = 1 \tag{A1}$$

is satisfied. Now, choose polynomials

$$v(z) = \frac{c_4\hat{x}(z) - c_3\hat{y}(z)}{c_1c_4 - c_2c_3}, \qquad w(z) = \frac{-c_2\hat{x}(z) + c_1\hat{y}(z)}{c_1c_4 - c_2c_3}$$

It is easy to show that the Bezout identity

$$v(z)[c_1a(z) + c_2b(z)] + w(z)[c_3a(z) + c_4b(z)] = 1$$

is satisfied. Thus, because $\deg [c_1a(z) + c_2b(z)] = \deg [c_3a(z) + c_4b(z)] = n$ and also $\deg v(z) < n$ and $\deg w(z) < n$, the polynomials $c_1a(z) + c_2b(z)$ and $c_3a(z) + c_4b(z)$ are coprime. □

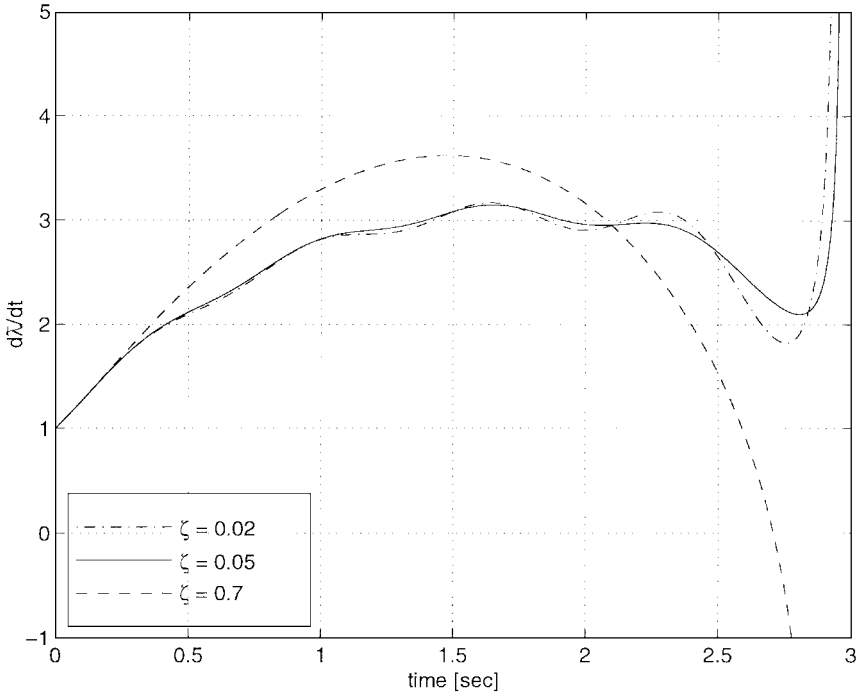

Fig. 10 Time history of $\bar{\dot{\lambda}} = \dot{\lambda}/\dot{\lambda}_0$ for a 5-g target maneuver with $t_f = 3$ s, $N' = 4$, $\tau_1 = 0.3$ s, $\omega_n = 10$ rad/s, $\dot{\lambda}_0 = 0.5$ deg/s, and $\zeta = 0.02$, 0.05, and 0.7.

Now, the proof of Lemma 1 is as follows. Consider first the polynomials $sq(s)$ and $p(s)$, where

$$sq(s) = N'n(s) - 2d(s), \qquad p(s) = d(s) \tag{A2}$$

Because $n(s)$ and $d(s)$ are coprime, by the Appendix Lemma $sq(s)$ and $p(s)$ are also coprime. Now, because $G(0) = 1$ and $N' \neq 2$, then $N'n(0) - 2d(0) \neq 0$ and, therefore, $q(s)$ and $p(s)$ are coprime. □

Appendix B: Proof of Eq. (38)

Consider the transfer function

$$G(s) = \prod_{i=1}^{n} \frac{1}{\tau_i s + 1}$$

Recall from Eqs. (27) and (28) that

$$\tau_0 = -N' \cdot \min_{\omega \neq 0} \mathrm{Re}\left[\frac{G(j\omega)}{j\omega}\right] \tag{B1}$$

Now, using the identity

$$\mathrm{Re}\left[\frac{G(j\omega)}{j\omega}\right] = \frac{1}{2}\left[\frac{G(j\omega)}{j\omega} - \frac{G(-j\omega)}{j\omega}\right] \tag{B2}$$

and substituting $G(j\omega)$ into Eq. (B2), we obtain after some algebraic manipulations

$$\mathrm{Re}\left[\frac{G(j\omega)}{j\omega}\right] = -\frac{1}{\omega}\left\{\frac{\mathrm{Im}\left[\prod_{i=1}^{n}(\tau_i j\omega + 1)\right]}{\prod_{i=1}^{n}\left[(\tau_i\omega)^2 + 1\right]}\right\} \tag{B3}$$

Also,

$$\mathrm{Im}\left[\prod_{i=1}^{n}(\tau_i j\omega + 1)\right] = \prod_{i=1}^{n}\sqrt{(\tau_i\omega)^2 + 1} \cdot \sin\omega \sum_{k=1}^{n}\tau_k \tag{B4}$$

Substituting Eq. (B4) into Eq. (B3) yields

$$\mathrm{Re}\left[\frac{G(j\omega)}{j\omega}\right] = -\frac{1}{\omega}\left[\frac{\left(\sin\omega\sum_{k=1}^{n}\tau_k\right)}{\prod_{i=1}^{n}\sqrt{(\tau_i\omega)^2 + 1}}\right] \tag{B5}$$

Note that

$$\lim_{\omega \to 0} \mathrm{Re}\left[\frac{G(j\omega)}{j\omega}\right] = -\sum_{k=1}^{n}\tau_k \tag{B6}$$

and

$$\frac{1}{\omega}\left[\frac{\left(\sin\omega\sum_{k=1}^{n}\tau_k\right)}{\prod_{i=1}^{n}\sqrt{(\tau_i\omega)^2 + 1}}\right] \leq \frac{1}{\omega}\sin\omega\sum_{k=1}^{n}\tau_k \leq \sum_{k=1}^{n}\tau_k \qquad \forall\omega > 0 \tag{B7}$$

Substituting Eq. (B7) into Eq. (B5) gives

$$\mathrm{Re}\left[\frac{G(j\omega)}{j\omega}\right] \geq -\sum_{k=1}^{n}\tau_k, \qquad \forall\omega > 0 \tag{B8}$$

therefore, by Eq. (B6)

$$\min_{\omega \neq 0} \mathrm{Re}\left[\frac{G(j\omega)}{j\omega}\right] = -\sum_{k=1}^{n}\tau_k, \qquad \tau_0 = N'\sum_{i=1}^{n}\tau_i \qquad \square$$

References

[1] Shneydor, N., "Proportional Navigation Guidance—A Survey," RAFAEL, Rept. MT/P/013/30/84, Haifa, Israel, May 1984.

[2] Guelman, M., "A Qualitative Study of Proportional Navigation," *IEEE Transactions on Aerospace and Electronic Systems*, Vol. AES-7, No. 4, 1971, pp. 637–643.

[3] Zarchan, P., *Tactical and Strategic Missile Guidance*, Vol. 124, Progress in Astronautics and Aeronautics, AIAA, Washington, DC, 1990, pp. 87–110; Chap. 5.

[4] Shinar, J., "Divergence Range of Homing Missiles," *Israel Journal of Technology*, Vol. 14, July 1976, pp. 47–55.

[5] Guelman, M., "The Stability of Proportional Navigation Systems," AIAA Paper 90-3380, July 1990.

[6] Rew, D. Y., Tahk, M. J., and Cho, H., "Short Time Stability of Proportional Navigation Guidance Loop," *IEEE Transactions on Aerospace and Electronic Systems*, Vol. 32, No. 4, 1996, pp. 1107–1115.

[7] Tanaka, T., and Hirofumi, E., "Hyperstable Range in Homing Missiles," AIAA Paper 90-3381, July 1990.

[8] Zarchan, P., "Complete Statistical Analysis of Nonlinear Missile Guidance Systems—SLAM," *Journal of Guidance and Control*, Vol. 2, No. 1, 1979, pp. 71–78.

[9] Curran, P. F., "Proof of the Circle Criterion for State Space Systems via Quadratic Lyapunov Functions—Part 1," *International Journal of Control*, Vol. 57, No. 4, 1993, pp. 921–955.

[10] Curran, P. F., "Proof of the Circle Criterion for State Space Systems via Quadratic Lyapunov Functions—Part 2," *International Journal of Control*, Vol. 57, No. 4, 1993, pp. 957–969.

[11] Sandberg, I. W., "A Frequency Domain Condition for the Stability of Feedback Systems Containing a Single Time-Varying Nonlinear Element," *Bell System Technical Journal*, Vol. 43, No. 4, 1964, pp. 1601–1608.

[12] Narendra, K. S., and Goldwyn, R. M., "A Geometrical Criterion for the Stability of Certain Nonlinear Nonautonomous Systems," *IEEE Transactions on Circuit Theory*, Vol. CT(11), No. 3, 1964, pp. 406–408.

[13] Luenberger, D. G., *Introduction to Dynamic Systems, Theory, Models and Applications*, Wiley, New York, 1979, pp. 126–152; Chap. 6.

[14] Vidyasagar, M., *Nonlinear System Analysis*, 2nd ed., Prentice–Hall, Englewood Cliffs, NJ, 1993, pp. 223–230; Chap. 5.